

Temporal Correlation of Pathology and DNA Damage With Gene Expression in a Choline-Deficient Model of Rat Liver Injury

Christine L. Powell,^{1,2} Oksana Kosyk,² Blair U. Bradford,² Joel S. Parker,³ Edward K. Lobenhofer,⁴ Ayumi Denda,⁵ Fumiyouki Uematsu,⁶ Dai Nakae,⁶ and Ivan Rusyn^{1,2}

Hepatocellular carcinoma (HCC) is the terminal event in chronic liver diseases with repeated cycles of cellular injury and regeneration. Although much is known about the cellular pathogenesis and etiological agents leading to HCC, the molecular events are not well understood. The choline-deficient (CD) model of rodent HCC involves the consecutive emergence of a fatty liver, apoptosis, compensatory proliferation, fibrosis, and cirrhosis that is markedly similar to the sequence of events typified by human HCC. Moreover, oxidative stress is thought to play a pivotal role in the progression of the disease. Here, we hypothesize that gene expression profiling can temporally mirror the histopathology and oxidative DNA damage observed with this model. We show that clusters of highly co-regulated genes representing distinct cellular pathways for lipid biosynthesis and metabolism, apoptosis, cell proliferation, and tissue remodeling temporally correlate with the well-defined sequential emergence of pathological alterations in the progression of liver disease. Additionally, an oxidative stress signature was observed that was corroborated in a time-dependent manner with increases in oxidized purines and abasic sites in DNA. Collectively, expression patterns were strongly driven by pathology, demonstrating that patterns of gene expression in advanced stages of liver disease are primarily driven by histopathological changes and to a much lesser degree by the original etiological agent. **In conclusion**, gene expression profiling coupled with the CD model of HCC provides a unique opportunity to unveil the molecular events associated with various stages of liver injury and carcinogenesis and to distinguish between causal and consecutive changes. *Supplementary material for this article can be found on the HEPATOLOGY website (<http://www.interscience.wiley.com/jpages/0270-9139/suppmat/index.html>).* (HEPATOLOGY 2005;42:1137-1147.)

Abbreviations: CD, choline-deficient/choline deficiency; HCC, hepatocellular carcinoma; HBV, hepatitis B virus; HCV, hepatitis C virus; CC, choline-sufficient L-amino acid defined; FDR, false discovery rate; SAM, Significance Analysis of Microarrays; GO, Gene Ontology; PC, phosphatidylcholine; PKC, protein kinase C; AP, apurinic/pyrimidinic; Ogg1, oxoguanine DNA glycosylase 1; 8-oxo-dG, 8-oxo-deoxyguanosine.

From the ¹Curriculum in Toxicology, School of Medicine, and the ²Department of Environmental Sciences and Engineering, School of Public Health, University of North Carolina, Chapel Hill, NC; ³Constella Health Sciences, Durham, NC; ⁴Paradigm Array Labs, Service Unit of Icoria, Inc., Research Triangle Park, NC; the ⁵Department of Molecular Pathology, Nara Medical University, Nara, Japan; and the ⁶Department of Pathology, Sasaki Institute, Sasaki Foundation, Tokyo, Japan.

Received February 9, 2005; accepted August 23, 2005.

Supported in part by grants from the National Institutes of Health (NIH): ES11391, ES11660, ES10126, CA52806 and CA82506; and Grants-in-Aid (14-9, 14-11) for Cancer Research from the Ministry of Health, Labor, and Welfare of Japan. I.R. was a recipient of a Transition to Independent Position award (ES11660) from the National Institute of Environmental Health Sciences (NIEHS). C.L.P. was supported, in part, by NIEHS Training Grant, T32-ES07126, from NIH.

The choline-deficient (CD) diet is an extensively studied non-chemical-induced, non-genotoxic model of rodent hepatocellular carcinoma (HCC) that produces a well-defined temporal pattern of pathological changes (Fig. 1). It is characterized by an initial increase in triglycerides resulting in macro-vesicular fat deposition (steatosis) that quickly diffuses throughout the entire liver within 4 to 5 days.¹ By 4 weeks, increased fat storage and oxidative stress are thought to contribute to hepatocellular injury, which prompts apoptosis² and is coupled with compensatory liver regenera-

Address reprint requests to: Ivan Rusyn, M.D., Ph.D., CB#7431, Department of Environmental Sciences and Engineering, University of North Carolina at Chapel Hill, Chapel Hill, NC 27599-7431. E-mail: iir@unc.edu; fax: 919-843-2596.

Copyright © 2005 by the American Association for the Study of Liver Diseases.

Published online in Wiley InterScience (www.interscience.wiley.com).

DOI 10.1002/hep.20910

Potential conflict of interest: Nothing to report.

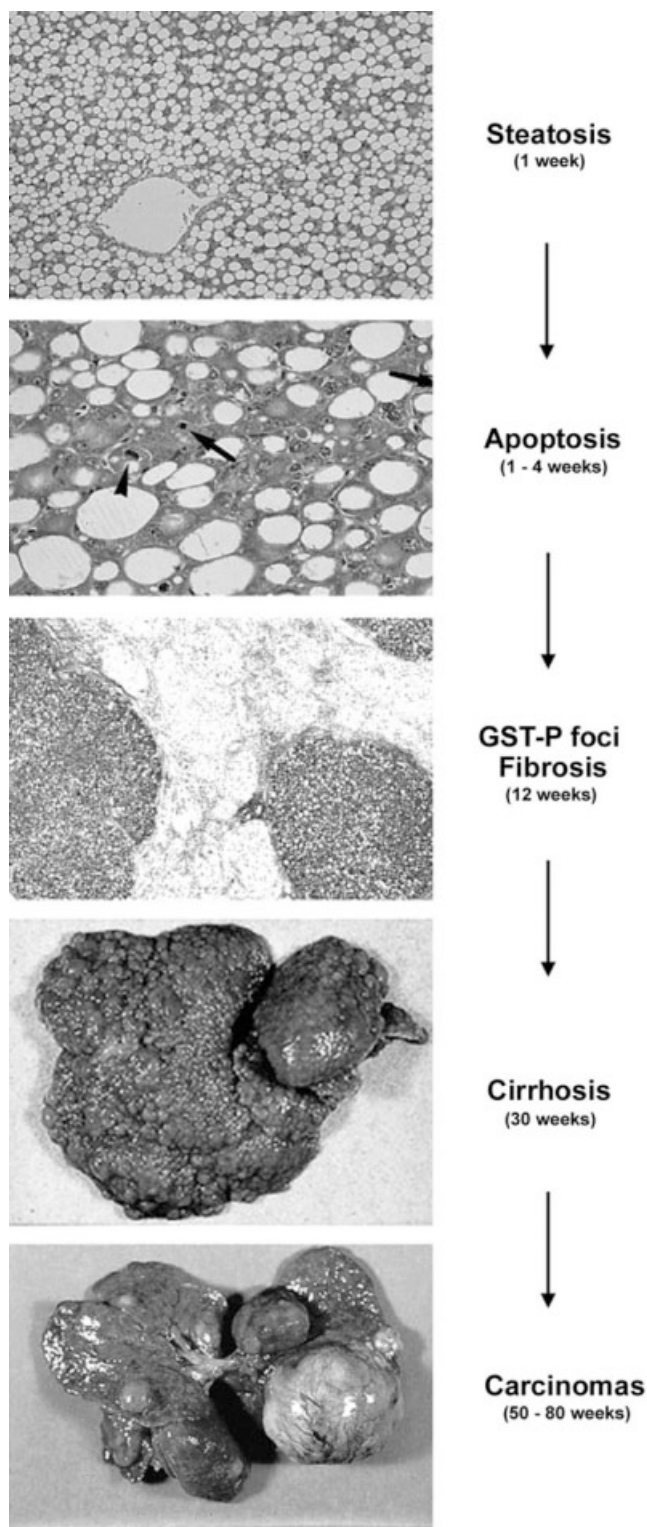


Fig. 1. Pathological stages of liver disease progression in a rat model of HCC. The choline-deficient L-amino acid-defined diet is a non-genotoxic model of rodent hepatocarcinogenesis. Choline deficiency produces a well-defined temporal pattern of histopathological changes, beginning with a fatty liver (steatosis), hepatocellular injury, apoptosis with compensatory proliferation, fibrosis, and cirrhosis. Pre-neoplastic foci with a glutathione S-transferase-positive (GST-P) phenotype eventually give rise to the development of hepatocellular adenomas and carcinomas within a year of administering the diet.

tion.³ Fibrosis develops as activated hepatic stellate cells increase collagen production, disrupting liver architecture, and eventually leads to cirrhosis by 30 weeks of treatment.⁴ Carcinomas develop, with a 100% incidence by 52 weeks.⁵ The sequence of pathological events is remarkably similar to the progression of human HCC associated with hepatitis B (HBV) and C (HCV) viral infections, non-alcoholic fatty liver disease, and alcohol abuse.

The development and progression of HCC in the CD model is not well understood because of the complexity of genetic and epigenetic events that occur in hepatocytes. Nevertheless, repeated cycles of hepatocyte injury and regeneration, oxidative stress to DNA,⁶ chronic activation of protein kinase C,⁷ activation of arachidonic acid cascade, in particular cyclooxygenase-2,⁸ and hypomethylation of *c-fos*, *c-myc*, and *c-Ha-ras*^{9,10} have been reported to occur. However, the definitive role of each of these processes in disrupting liver homeostasis and progression to HCC has yet to be elucidated.

Molecular profiling of cancer by high-density microarray analysis is a powerful tool for identifying new biomarkers with diagnostic and predictive value as well as increasing our understanding of the mechanisms of carcinogenesis.¹¹ Genomic studies of breast, lung, and colon cancers have identified unique gene networks and regulatory pathways useful in classifying tumors into clinically relevant sub-types.¹²⁻¹⁴ Furthermore, the corroboration of altered expression patterns with phenotypic endpoints such as histology, pathology, and clinical chemistry have provided the much-needed validation of molecular profiling data.¹⁵

HCC is the fifth leading cause of cancer death worldwide. Early diagnosis is difficult because most people are asymptomatic during the early stages of the disease, and there are no diagnostic markers currently available, contributing to the high mortality rate. Moreover, the lack of appropriate and reproducible animal models for HCC impedes the development of diagnostic markers and therapies. Transcriptional profiling coupled with an appropriate animal model for HCC provides an opportunity to identify novel molecular markers with diagnostic and prognostic value. Here, we show that gene expression profiling of CD model of HCC can be phenotypically anchored to the well-defined sequential emergence of histopathological changes and associated oxidative stress to DNA. The gene expression changes observed with this model are remarkably similar to human HCC expression data from diverse etiologies. Collectively, the expression patterns in advanced liver disease are strongly driven by pathological conditions rather than causes. Thus, under-

standing the early molecular events leading to such events is key for medical intervention.

Materials and Methods

Animals and Treatments. The studies detailed herein were performed using tissue samples (stored at -80°C) from a previously published report¹⁶ in which male Fisher 344 rats were administered either a choline-sufficient L-amino acid–defined (CS) diet, or CD L-amino acid–defined diet and water *ad libitum* for 12, 30, or 80 weeks; or samples generated specifically for this study (3 days and 4 weeks) using the identical procedure.

RNA Isolation. Total RNA was isolated using RNeasy kit (Qiagen, Valencia, CA). Samples were stored at -80°C until assayed. The quality of preparations was determined using Bio-Analyzer (Agilent Technologies, Palo Alto, CA).

Microarray Experiments. Gene expression analysis of isolated RNA from liver tissue was performed using Affymetrix Rat 230A microarrays (Affymetrix, Santa Clara, CA) at the Functional Genomics Core at UNC-CH using standard procedures specified by the manufacturer (neuroscience.unc.edu/core_facilities/functional/).

Microarray Data Analysis. Preliminary analysis was performed using MAS 5.0 software (Affymetrix). Array quality was determined by examination of 3' to 5' intensity ratios of selected genes. Data was normalized to global probe intensity using a robust multi-array average method,¹⁷ and expression data were \log_2 -transformed and gene-median centered. Hierarchical clustering analysis was conducted using Cluster (rana.lbl.gov/EisenSoftware.htm) to perform gene-centered, average-linkage clustering¹⁸; the data were visualized using Java TreeView (jtreeview.sourceforge.net).

Two independent statistical tests were applied to identify the unique gene expression profiles of CD and CS. First, the method of Sorlie et al.¹⁹ was used to define genes intrinsic to an experimental group versus control, where a group is defined as a unique combination of the type of diet (CD or CS) and duration of treatment (4, 12, 80 weeks and tumors). This method gives the best (lowest) scores to those genes whose variation is low within a group, but high across multiple groups. The resulting list is expected to encompass subsets of genes whose expression is common to all samples within each group. To establish a false discovery rate (FDR) for this computational approach (*i.e.*, to establish statistical significance), the group label for each sample was randomly permuted and the set of intrinsic scores was calculated from the resulting groupings. This process was repeated 20 times.

A threshold of the intrinsic scores was determined by identifying the score that gave the greatest number of significant calls with less than 5% occurrence in the permuted results. In addition, a two-class, unpaired significance analysis of microarrays (SAM²⁰) was performed as described for intrinsic gene identifier. The SAM algorithm differs from the intrinsic scores defined previously because more weight is placed on differences in fold changes between the groups. Delta values were adjusted to obtain the gene list with a $<5\%$ FDR. All microarray raw data tables are available at the UNC Microarray Database (genome.unc.edu).

RNase Protection Assays. Expression of base excision DNA repair genes was analyzed using RNase protection assay with rat multi-probe template set (rBER, BD PharMingen, San Diego, CA) as described elsewhere.²¹

Detection of Apurinic/Apyrimidinic Sites and Oxidized Purines. Genomic DNA was extracted by a procedure slightly modified from the method reported previously.²² To minimize formation of oxidative artifacts during isolation, 2,2,6,6-tetramethylpiperidinoxyl (20 mmol/L) was added to all solutions, and all procedures were performed on ice. The apurinic/apyrimidinic (AP) and OGG1 slot blot assays were performed as previously described.^{23,24}

Results and Discussion

Hierarchical Analysis of Gene Expression Data Distinguishes CS- and CD-Treated Groups. It has been well established that a CD diet causes HCC in rats and produces a well-defined temporal pattern of pathological changes involving steatosis, hepatocyte injury, fibrosis, and cirrhosis (Fig. 1). To assess whether expression profiling temporally mirrors the altered pathological changes observed with the liver disease induced by this treatment, we applied a high-throughput Affymetrix Rat 230A array to liver tissues from CS (control) or CD diet-fed Fisher 344 rats (Supplemental Fig. 1). Liver tissues were chosen at 4, 12, and 80 weeks, as were tumors larger than 5 mm at 80 weeks, to reflect the various stages of liver injury. The gene expression profiling was performed on whole liver, making it difficult to discern the contribution of individual cell types. Furthermore, 30- and 80-week liver samples may not be devoid of tumors 5 mm or less and may contain necrotic and apoptotic hepatocytes in addition to other cell types associated with cirrhosis.

Identification of Gene Clusters Temporally Expressed in Liver of CD-Treated Rats. Two independent statistical tests, intrinsic gene identifier¹³ and SAM,²⁰ were performed to identify genes whose expres-

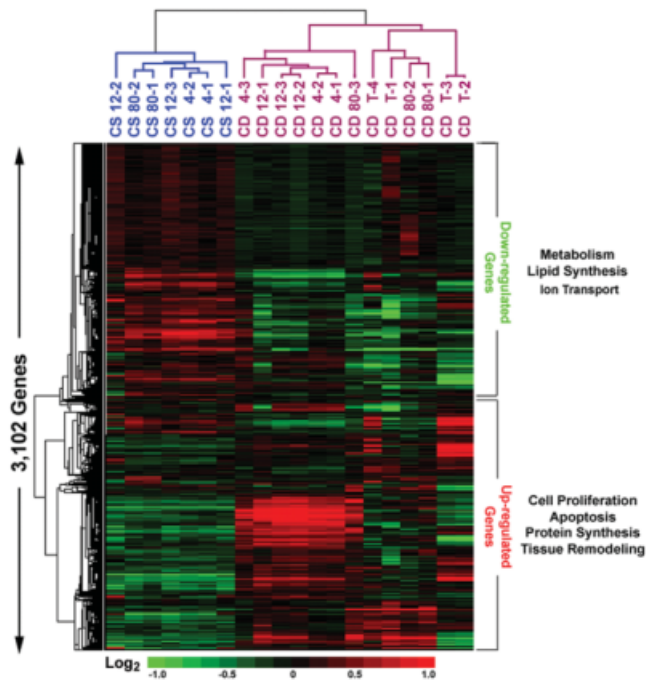


Fig. 2. Hierarchical clustering of choline-sufficient (CS) and choline-deficient (CD) liver samples using "intrinsic" gene set. Intrinsic analysis identified genes whose expression levels vary the least within a single treatment group but are highly variable between treatments (FDR < 5%). Hierarchical clustering analysis was conducted on a list of 3,100 non-redundant genes identified through such analysis. Functional classes were assigned to each gene using Gene Ontology (GO) and revealed that the highly upregulated genes were related to cell proliferation, apoptosis, protein synthesis, and tissue remodeling, whereas downregulated genes were related to metabolism, lipid synthesis, and ion transport. For unsupervised hierarchical clustering of the entire rat array, see Supplemental Fig. 1.

sion profiles were unique to CD at any time using the 6,045 fully annotated transcripts on the array. Intrinsic gene identifier analysis showed that expression levels of 3,102 genes segregated at least a single time (e.g., 4, 12, 80 weeks, or tumors) compared with its corresponding control group. SAM identified 4,673 genes, of which 88% (2,739 genes) were also detected by an intrinsic gene identifier analysis. Genes from both lists were assigned into functional categories using Gene Ontology (GO) and enriched KEGG pathways using Onto-Pathway-Express.²⁵ Considerable overlap between the two methods was observed, as the enriched KEGG pathways identified by both analyses were identical (Supplemental Fig. 2; Supplementary material for this article can be found on the HEPATOLOGY website: <http://www.interscience.wiley.com/jpages/0270-9139/suppmat/index.html>).

The intrinsic gene list was subjected to clustering analysis using a centered, average-linkage hierarchical algorithm. The resulting dendrogram (Fig. 2) showed two major branches separating the experimental groups, CS and CD. Heterogeneity between tumor samples was ob-

served, with T2 and T3 samples (two distinct tumors from the same animal) being similar to each other but somewhat different from other tumors and 80-week CD samples. Data mining using GO annotations for intrinsic genes (NetAffx Analysis Center, affymetrix.com) was used to assign functional classes and to determine the cellular and molecular pathways defining treatment separation. Several clusters of highly upregulated genes evoked by CD were associated with apoptosis, cell proliferation, protein synthesis, and tissue remodeling. Conversely, metabolism, lipid synthesis, and ion transport pathways were selectively downregulated compared with CS.

To determine whether molecular profiling would model the temporal changes in histopathology observed with CD, genes with a functional assignment associated with lipid biosynthesis or metabolism (excluding ion transport pathways), apoptosis, cell proliferation, and tissue remodeling were compiled. Supervised hierarchical clustering was conducted to view temporal changes in expression of genes associated with the previously mentioned biological processes (Fig. 3, Supplemental Table 1). This result demonstrates that dramatic alterations in gene expression occur as early as 4 weeks in CD samples.

Gene Expression Patterns Reveal CD Attributes to Altered Lipid Metabolism. Accumulation of lipid mostly comprised of triglycerides occurs in hepatocytes within days of administering a CD diet to rats.²⁶ This has been attributed to the compromised ability to synthesize phosphatidylcholine (PC), a major constituent of lipoprotein envelopes, whereby secretion of triglycerides from the liver is inhibited. PC plays a major role as a structural component of cellular membranes, and as a source of second messengers, it can influence both normal physiological and pathological processes, including carcinogenesis.

Indeed, GO-assisted search identified 160 genes within the intrinsic gene list with a functional assignment to either lipid biosynthesis or metabolism (Fig. 3A). After 4 weeks of CD diet, an induction of genes for fatty acid (Cpt1a, Cte1, Fabp2, Fads1, and Mte1) and cholesterol (Apoa1, Abcg1, and Vldlr) metabolism occurred, most likely as a result of the accumulation of intracellular lipids. At 12 weeks, there was an additional increase in expression of phospholipases (Pla2g4a, Plce1, Pspla1, and Dpep1) that release second messengers and metabolic precursors from membrane phospholipids. For example, activation of membrane receptors coupled to phospholipase C release 1,2-*sn*-diacylglycerol from intact membrane phospholipids, which are potent activators of protein kinase C (PKC). PKC targets include proteins involved in the control of gene expression, cell division, and differentiation,²⁷ and alterations in PKC signaling

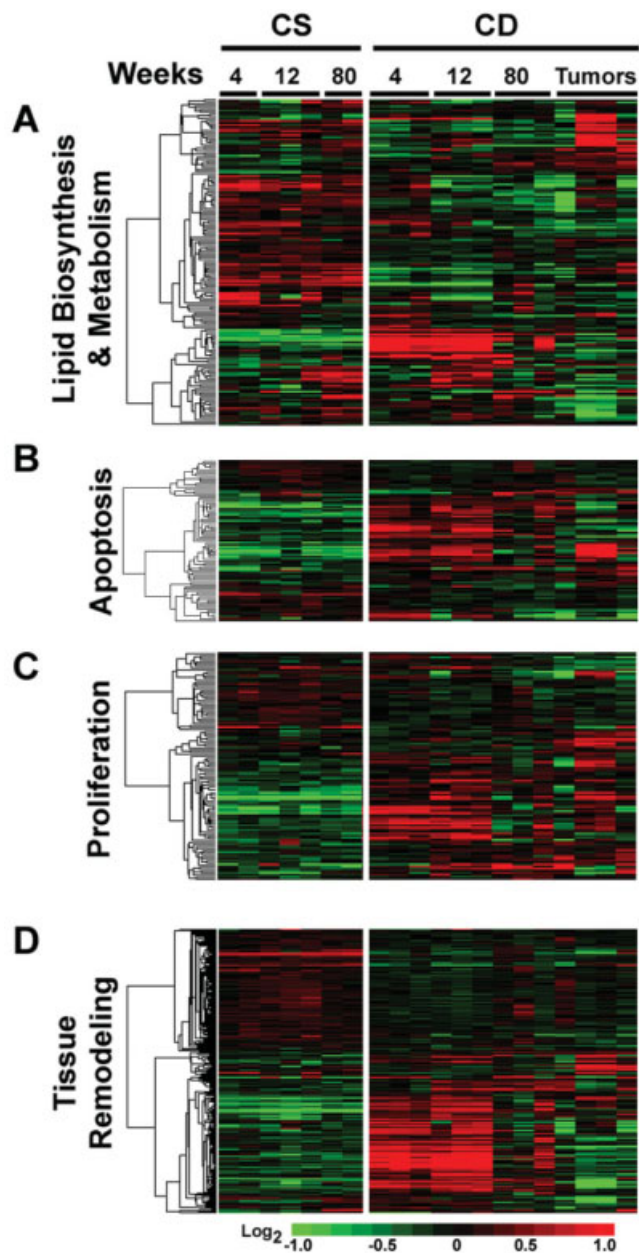


Fig. 3. Supervised hierarchical clustering of altered cellular and molecular pathways associated with choline deficiency. Gene Ontology (GO) was used to assign functional classes to an "intrinsic" gene set to identify cellular pathways related to the histopathological events evoked by choline deficiency. These cellular pathways include lipid biosynthesis and metabolism (A), apoptosis (B), cell proliferation (C), and tissue remodeling (D).

have been attributed to tumorigenesis.²⁸ Interestingly, CD rats accumulate high levels of 1,2-*sn*-diacylglycerol in cellular membranes, and this coincides with increased PKC levels and activity.⁷ Phospholipase A2 releases arachidonic acid from cellular phospholipids, a precursor to the biologically potent eicosanoids, prostaglandins, and thromboxanes, of which several members were highly expressed (Ptgfrn, Ptgs1, Tbxas1, Ltc4s). At 80 weeks, an

increase in expression of phospholipases (Plcg1 and Pla2g6) and phosphoesterases (Pde4b and Pter) occurred. Over the course of the CD diet, a transient downregulation of genes associated with steroid and fatty acid synthesis and lipid transport occurred (Supplemental Table 1).

Gene Expression Patterns Show That CD Activates Apoptotic Pathways. Numerous reports exist of induction of apoptosis with the CD diet through both p53-dependent and -independent pathways. Supervised hierarchical clustering of genes associated with apoptosis showed a strong induction of pro-apoptotic genes at 4 weeks of CD diet (Fig. 3B) such as caspases, apoptosis activating factor 1 (APAF1), tissue necrosis factor, and p53. Tumor samples did not express p53 or mitochondrial-mediated apoptotic genes such as APAF1 and caspases; however, a small number of genes upregulated in tumor samples were associated with death receptor-mediated pathway, including tumor necrosis factor and nerve growth factor receptor superfamilies and Cflar.

In vitro studies with CWSV-1 rat hepatocytes have shown that the rate of apoptosis is inversely correlated with cellular PC content.² Moreover, inhibition of PC biosynthesis by CD diet leads to apoptosis by an increase in intracellular ceramide levels in neurons²⁹; however, our data show an increase in expression of genes related to ceramide metabolism, including acid ceramidase and uridine-diphosphoglucuronate-glucose ceramide glucosyltransferase, suggesting that ceramide is not an important mediator of apoptosis in this model. Additionally, the induction of apoptotic genes coincided with a predominance of genes associated with positive regulators of the cell cycle (Fig. 3C, Supplemental Table 1) such as cyclins, oncogenes, and cyclin dependent kinases.

Gene Expression Patterns Reveal CD Mediates Tissue Repair Through Activation of Hepatic Stellate Cells. Recurrent hepatocellular injury is a hallmark of the CD diet that chronically activates cellular and molecular mechanisms of tissue repair, leading to fibrosis and cirrhosis. Analysis of gene expression patterns revealed a highly expressed cluster of genes related to the initiation and promotion of fibrosis at 4 and 12 weeks of CD treatment (Fig. 3D), including transforming growth factor beta, which promotes the proliferation of fibroblasts and hepatic stellate cells and the extracellular matrix components collagens, proteoglycans, fibronectin, laminins, and matrix metalloproteinases.^{30,31} Moreover, hepatic stellate cell-specific genes were upregulated, including stellate activation associated cell protein, alpha-smooth muscle actin, vimentin, and tissue inhibitors of metalloproteinases, supporting their involvement in fibrosis.^{32,33}

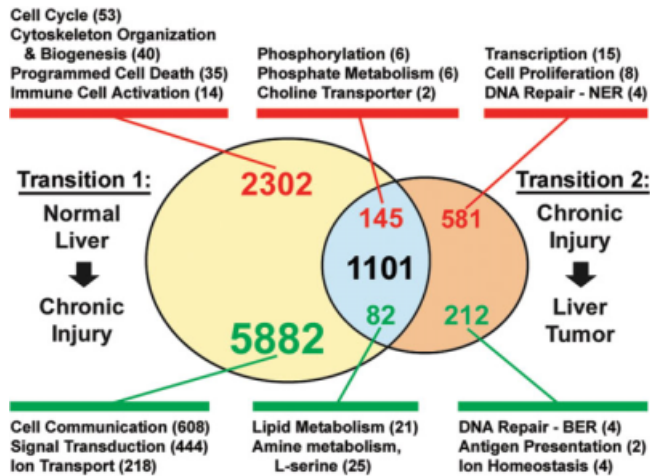


Fig. 4. Venn diagram illustrating the distribution of gene alterations between liver injury transition states in choline-deficient rats. Significant gene lists were generated using SAM (FDR < 5%) for each transition state as described in text and cross-compared. Values represent the number of genes significantly induced (red) or repressed (green) that are either unique or shared by the 2 transition states. Between the 2 injury states, 1,101 genes were shared, but their expression changes were directionally opposite. Gene lists were submitted to GoMiner³⁴ to identify significantly enriched biological processes ($P < .05$), of which a few are shown. The number of genes associated with each process is given in parentheses. A complete listing of enriched biological processes is available in Supplementary Table 2.

Gene Expression Reveals Liver Injury Transition States in CD Rats. We have identified gene clusters that temporally mirrored the histopathological alterations observed with the CD model in rat liver. Here, we examined the genes associated with the initial transition from normal liver to a state of chronic liver injury that ultimately leads to the second transition to HCC. To define these two major transition states, we performed unpaired SAM analysis between CS samples versus CD non-tumor samples (*i.e.*, transition state 1), and CD non-tumors versus CD tumors (*i.e.*, transition state 2). Next, to cross-compare these genes lists, we generated a Venn diagram (Fig. 4) to identify genes that are shared or unique in these two liver injury transition events. Lastly, the gene lists were submitted to GoMiner³⁴ to identify significantly enriched biological processes (Supplemental Table 2).

SAM analysis of expression changes during transition state 1 identified 2,302 and 5,882 genes to be significantly upregulated or downregulated, respectively. GO mapping found a significant enrichment in biological processes related to proliferation, cell death, and tissue remodeling. In contrast, processes related to cell communication, in particular, G-protein coupled signal transduction and ion transport pathways, were significantly downregulated, most likely a reflection of the loss of cell membrane structure caused by the inability to synthesize

phospholipids. For transition state 2, SAM identified 581 and 212 genes to be significantly upregulated or downregulated, respectively. Processes related to cell proliferation alongside with transcription-coupled nucleotide excision repair were significantly increased. In contrast, processes related to oxidative DNA damage and repair and apoptosis were downregulated, potentially signifying increased genomic instability and survival of cells in liver tumors.

Interestingly, 1,101 genes were shared between the two transition states, but their expression changes were directionally opposite. Specifically, 518 and 583 genes were significantly upregulated or downregulated in transition state 1 and vice versa. A number of processes related to cell motility, cytoskeleton reorganization, and immune response were upregulated in transition state 1, a reflection of the underlying molecular events that occur after extensive cellular injury. In contrast, transition state 2 showed a significant enrichment in metabolic processes that would be required to sustain tumor growth.

CD-Induced Hepatocarcinogenesis Is Preceded by Oxidative Stress to DNA. Treatment of rodents with a CD diet causes oxidative stress to DNA that is predominantly removed and repaired by the base excision repair pathway. To confirm that oxidative stress to DNA is present in CD rats, changes in expression of DNA repair genes, a sensitive *in vivo* marker of oxidative stress to DNA,³⁵ was evaluated. A significant increase in expression of proliferating-cell nuclear antigen, AP endonuclease 1, 8-oxoguanine DNA glycosylase 1 (Ogg1), and polymerase beta was observed in CD-fed animals (Table 1). Additionally, expression of *O*⁶-methylguanine-DNA methyl transferase, an enzyme involved in the direct repair of alkylated guanine residues, was enhanced. Previous reports have shown increases in DNA methyl transferase expression with preneoplastic and neoplastic livers of rodents fed a CD diet, which is the result of a hypomethylated promoter.³⁶

In parallel, the intrinsic gene list for GO functional assignments associated with oxidative stress was examined and identified 92 genes. Hierarchical clustering of these genes showed a temporal separation of genes that are overexpressed in liver at 4 and 12 weeks, 12 and 80 weeks, and tumor samples (Fig. 5). The 4- and 12-week cluster reflects an upregulation of cellular antioxidant defenses such as heat shock protein (Hspa1b, Hspcb, Hsp60, and Hspa1a) and glutathione peroxidase (Gpx2 and Gpx3) genes. At 12 and 80 weeks, an increase in genes linked to DNA damage including the DNA repair genes apurinic/apyrimidinic endonuclease 1, DNA polymerase delta, and the DNA-damage-inducible transcript 4 was observed. Surprisingly, the expression of Ogg1 was not in-

Table 1. Expression of DNA Repair Genes in Rat Liver After Treatment With Control Choline-Sufficient (CS) or Choline-Deficient (CD) Diets

DNA Repair Genes	1 Week		12 Weeks		80 Weeks	
	CS	CD	CS	CD	CS	CD
<i>OGG1</i> , 8-oxoguanine DNA glycosylase 1	1.6 ± 0.1	1.9 ± 0.1*	1.9 ± 0.4	2.6 ± 0.5	0.9 ± 0.9	2.6 ± 0.4*
<i>MPG</i> , N-methylpurine DNA glycosylase	3.2 ± 2.9	2.0 ± 0.2	2.0 ± 1.2	3.1 ± 0.8	1.0 ± 0.2	5.2 ± 3.4
<i>APE</i> , apurinic/aprimidinic endonuclease 1	6.6 ± 0.7	8.4 ± 1.0	7.5 ± 2.2	12.3 ± 5.1	4.3 ± 0.1	13.8 ± 3.6*
<i>Pol β</i> , polymerase (DNA directed) β	5.6 ± 1.2	4.8 ± 0.7	4.5 ± 1.2	8.6 ± 2.1*	3.8 ± 0.9	9.5 ± 5.2
<i>PCNA</i> , proliferating cell nuclear antigen	4.4 ± 0.7	8.6 ± 3.2	4.4 ± 1.6	12.4 ± 5.1*	3.9 ± 1.7	8.1 ± 3.1
<i>PARP</i> , poly (ADP-ribose) polymerase	10.6 ± 1.2	10.6 ± 0.1	10.4 ± 2.8	14.0 ± 3.5	7.8 ± 1.9	9.7 ± 2.6
<i>MGMT</i> , O ⁶ -methylguanine DNA methyltransferase	13.1 ± 1.5	17.3 ± 0.9*	14.0 ± 3.5	27.5 ± 8.7*	19.4 ± 1.2	33.5 ± 13.2*

NOTE. RNase protection assay was performed on total RNA isolated from liver samples. The results are mean ± standard deviation from 3 animals per group. The relative expression of each gene was normalized to the expression of the housekeeping gene L32.

*Statistical difference ($P < .05$) from a corresponding CS group using Student *t* test.

creased in the microarray data; however, the concordant temporal upregulation of a number of DNA repair genes with CD is evidence of a biological response for oxidative DNA damage in this model.

In tumors, an upregulation in DNA repair genes including mismatch repair protein, polymerase epsilon, and mediator of DNA damage checkpoint 1 was found. Additionally, a number of cellular antioxidants were upregulated, including thioredoxins and glutathione S-transferases. Interestingly, thioredoxins have been demonstrated to promote proliferation and growth of tumors through induction of growth factors and cytokine activity.³⁷

Although previous reports have documented the accumulation of 8-oxo-dG DNA adducts in liver of rats given a CD diet, the data must be interpreted with caution because previous reports may be erroneous because of *ex vivo* oxidation during DNA isolation, as reported by the European Standards Committee on Oxidative DNA Damage.³⁸ Thus, we measured oxidized purines in DNA using an isolation procedure that was shown to minimize artifactual *ex vivo* oxidation. Figure 6A illustrates that background level of oxidized purines was below 1×10^6 nucleotides, in agreement with European Standards Committee on Oxidative DNA Damage–reported values.³⁹ Significant increases in oxidized purines were observed in animals given CD diet for 12 weeks and in tumor samples. Abasic sites in DNA are generated spontaneously by chemical depurination of labile oxidized bases and enzymatically by DNA glycosylases. To determine whether the number of mutagenic and clastogenic AP sites is increased after CD treatment, AP sites were measured. Significant increases (>2.5-fold) in the num-

ber of AP sites were seen in 12- and 30-week CD-treated rat liver (Fig. 6B).

Generation of oxidants and the resulting state of oxidative stress in the cell induces both genotoxic and epigenetic events that can promote the process of carcinogenesis. Oxidative stress to DNA is one of the earliest changes observed in rodent liver on a CD diet, with accumulations of 8-oxo-deoxyguanosine (8-oxo-dG), a mutagenic lesion capable of G:C to T:A transversions.^{40,41} Additionally, end products of lipid peroxidation such as malondialdehyde and 4-hydroxy-2-nonenal have been reported to form in liver of CD-treated animals,¹ resulting in exocyclic DNA adducts that are known to be mutagenic and genotoxic, respectively.⁴² Here, we have demonstrated that gene expression profiling revealed differential expression of oxidative stress-related genes for CD. Specifically, microarray expression data showed an induction of several DNA repair genes involved in the base excision repair pathway after 12 weeks' CD treatment and beyond, suggesting that DNA damage had occurred. This was confirmed with increases in AP and oxidized purines in liver DNA. The increase in expression of DNA repair genes and the accumulation of DNA lesions at 12 weeks corresponds to the development of fibrosis and cirrhosis. Recent studies demonstrated a correlation between increases in DNA repair expression and the histological stage of fibrosis in liver biopsies.⁴³ Moreover, increases in 8-oxo-dG adducts and expression of DNA repair genes was reported in the surrounding tissue of liver tumors.⁴⁴ Thus, the fibrotic process may be a contributing factor to the transformation of hepatocytes toward a neoplastic phenotype.

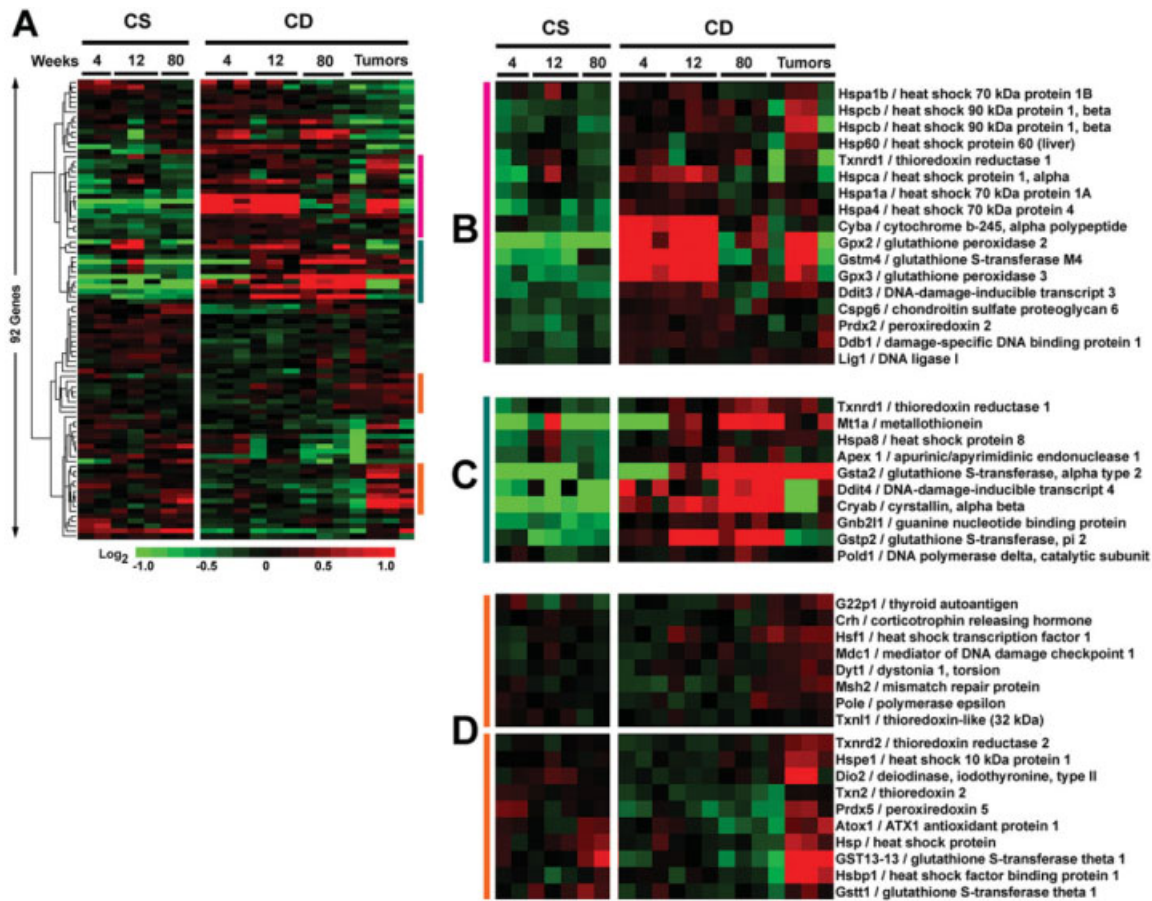


Fig. 5. Temporal expression of oxidative stress genes in rat liver evoked by a choline-deficient diet. Gene Ontology (GO) identified 92 genes within the "intrinsic" gene set associated with oxidative stress from rat liver samples treated with a control choline-sufficient (CS) or choline-deficient (CD) diet for 4 to 80 weeks. Tumor (T) samples were collected from CD-treated rats at 80 weeks. Supervised hierarchical clustering was conducted and is shown in A. Colored bars on right side of A illustrate the location of clusters shown in B-D. The clusters of temporally expressed genes expanded for 4 and 12 weeks (B), 12 and 80 weeks (C), and tumor samples (D).

CD-Induced Rat HCC and Human HCCs Are Similar at the Level of Gene Expression. To determine how the CD model of rat HCC recapitulates human HCC, gene expression patterns with data from a human HCC study⁴⁵ were compared. This study encompassed 102 primary liver tumors and 74 non-tumor liver samples. For this comparison, Ensembl genome browser (ensembl.org) was used to identify rat and human gene orthologs that were present on both microarray platforms. Of the 2,121 genes that were identified as differentially expressed in CD-induced tumors (*i.e.*, transition state 2), 492 orthologous genes were selected. Gene expression ratios were standardized to a mean \pm SD of 0 ± 1 in each data set. Hierarchical clustering analysis of the integrated data sets (Fig. 7) showed two major clusters, one representing human and CD rat HCC samples, and the other, with a few exceptions, representing non-tumor human liver tissues. Tumors from humans with HBV, HCV, as well as non-infected individuals, were interspersed within

the HCC cluster. Furthermore, two distinctive nodes with highly expressed genes were evident in HCC samples as compared with non-tumor liver tissue. Biological processes that were enriched in these nodes were identified using GO mapping. These included angiogenesis, cell-matrix adhesion, G-protein and tyrosine kinase signaling cascades, and protein metabolism. Thus, these data suggest that gene expression changes in CD-induced tumors in rats are similar to human HCC gene expression phenotype and may be potentially used to distinguish between human tumor and non-tumor samples.

Gene Expression Distinguishes Between Causal and Consecutive Events in Liver Disease. Although much is known about the cellular pathogenesis and etiological agents leading to HCC; the molecular events that contribute to the disease are not well understood. Thus, the use of appropriate animal models coupled with global gene expression profiling can provide the opportunity to serially dissect the molecular events associated with liver injury

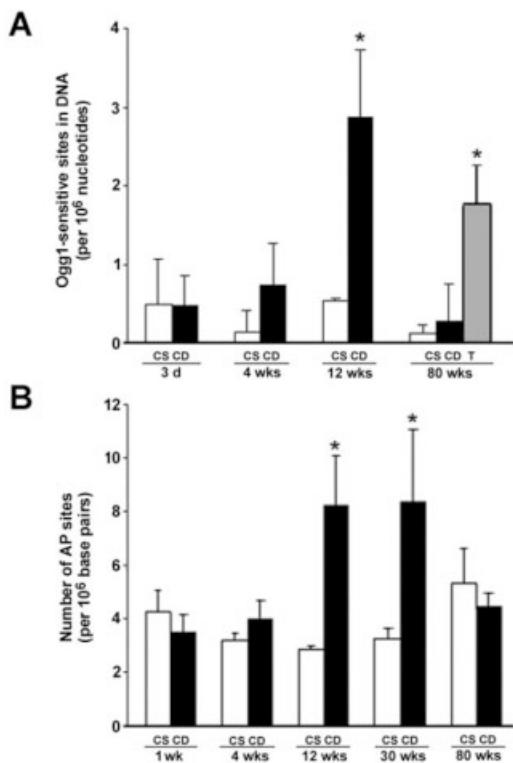


Fig. 6. Choline deficiency promotes the accumulation of oxidative DNA lesions in rat liver. Genomic DNA was isolated from livers of control CS diet (white square) and CD (black square) treated rats, and tumors (gray square) and the number of (A) Ogg1-sensitive sites (B) or apurinic/aprimidinic (AP) sites (B) determined as described in "Materials and Methods." Data are presented as means \pm standard deviation from 2 to 3 animals per group. *Statistical difference ($P < .05$) from corresponding control group by Student *t* test.

and disease. Here, we have demonstrated that microarray gene expression data can be phenotypically anchored to the sequential pathological alterations observed during the development of rodent HCC induced by a CD diet. The hierarchical clustering analysis of this expression data set was strongly driven by the histopathological changes that are observed during the progression of HCC by CD diet. Thus, these data provide the opportunity to decipher the genomic changes required to elicit such phenotypic endpoints.

Because the liver pathological changes observed in rodents on a CD diet are similar to that observed by agents (*e.g.*, HBV, HCV, and alcohol) causing chronic human liver injury, we suggest that similar expression patterns would be observed in advanced stages of human liver disease regardless of etiology. Indeed, gene expression patterns of CD-induced liver tumors are phenotypically similar to human HCC from diverse etiologies (*i.e.*, HBV-, HCV-, and HBV-/HCV-negative individuals). The fact that these liver tumors were interspersed among each other within the HCC branch demonstrates that, regardless of the initial confounding etiological agent, eventually these diseases converge onto a common and indistinguishable phenotype.

In conclusion, we have shown that gene expression profiling can temporally model the well-defined sequential emergence of pathological conditions and oxidative stress observed with the CD model of rodent HCC. Moreover, the development of fibrosis and cirrhosis tem-

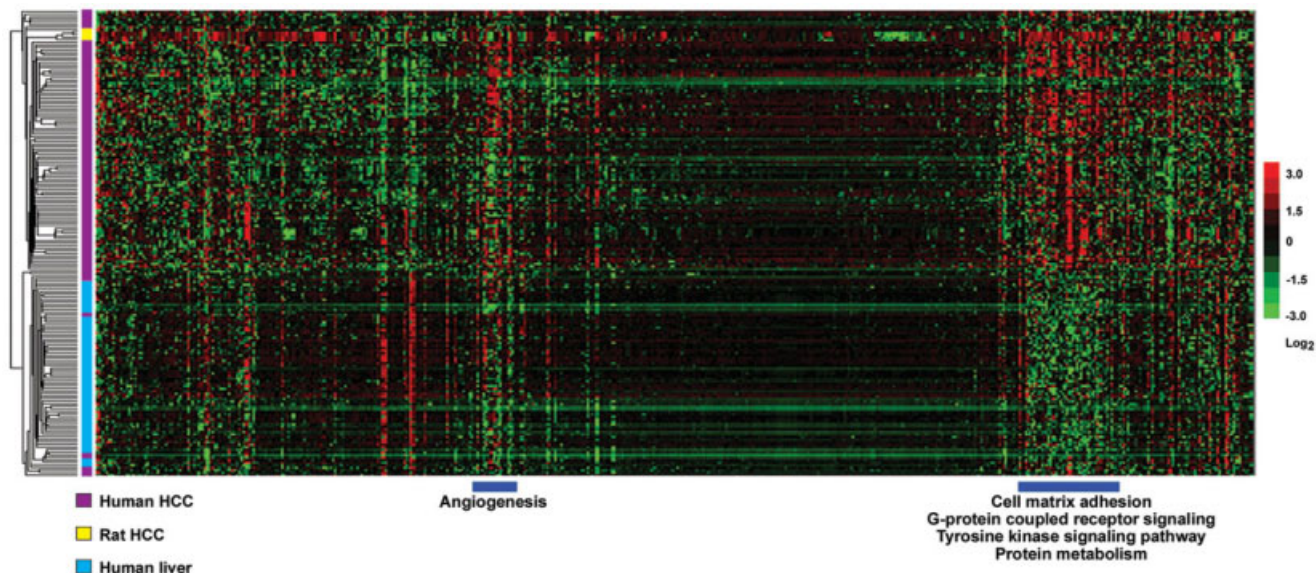


Fig. 7. Clustering analysis of rat and human hepatocellular carcinomas (HCCs). Unsupervised hierarchical cluster analysis of integrated rat (this study) and human⁴⁵ HCC datasets. Ensembl genome browser was used to identify orthologous genes present on both arrays (492 genes), and expression ratios were standardized to a mean \pm SD of 0 ± 1 before clustering. The two areas highlighted on the heatmap represent clusters of genes that are highly expressed in both rat and human HCC. Biological processes associated with these gene clusters are shown. A complete list of genes is available in Supplementary Table 3.

porally coincided with the accumulation of oxidative DNA lesions, processes that may contribute to hepatocyte transformation. Molecular profiling of tumors will not identify the early molecular changes required for transformation; however, the CD model of HCC in the rat provides an opportunity to serially dissect the molecular events related to the onset of liver injury and carcinogenesis that is also relevant to progression of human HCC.

Acknowledgment: The authors thank Dr. Jun Nakamura with the University of North Carolina-Chapel Hill for providing reagents for AP and OGG1 slot blot assays.

References

- Nakae D. Endogenous liver carcinogenesis in the rat. *Pathol Int* 1999; 49:1028-1042.
- Zeisel SH, Albright CD, Shin OH, Mar MH, Salganik RI, da Costa KA. Choline deficiency selects for resistance to p53-independent apoptosis and causes tumorigenic transformation of rat hepatocytes. *Carcinogenesis* 1997;18:731-738.
- Chandar N, Amenta J, Kandala JC, Lombardi B. Liver cell turnover in rats fed a choline-devoid diet. *Carcinogenesis* 1987;8:669-673.
- Ghoshal AK, Farber E. Liver biochemical pathology of choline deficiency and of methyl group deficiency: a new orientation and assessment. *Histol Histopathol* 1995;10:457-462.
- Nakae D, Yoshiji H, Mizumoto Y, Horiguchi K, Shiraiwa K, Tamura K, et al. High incidence of hepatocellular carcinomas induced by a choline deficient L-amino acid defined diet in rats. *Cancer Res* 1992; 52:5042-5045.
- Floyd RA, Kotake Y, Hensley K, Nakae D, Konishi Y. Reactive oxygen species in choline deficiency induced carcinogenesis and nitron inhibition. *Mol Cell Biochem* 2002;234-235:195-203.
- da Costa KA, Cochary EF, Blusztajn JK, Garner SC, Zeisel SH. Accumulation of 1,2-sn-diradylglycerol with increased membrane-associated protein kinase C may be the mechanism for spontaneous hepatocarcinogenesis in choline-deficient rats. *J Biol Chem* 1993;268:2100-2105.
- Endoh T, Tang Q, Denda A, Noguchi O, Kobayashi E, Tamura K, et al. Inhibition by acetylsalicylic acid, a cyclo-oxygenase inhibitor, and p-bromophenacylbromide, a phospholipase A2 inhibitor, of both cirrhosis and enzyme-altered nodules caused by a choline-deficient, L-amino acid-defined diet in rats. *Carcinogenesis* 1996;17:467-475.
- Dizik M, Christman JK, Wainfan E. Alterations in expression and methylation of specific genes in livers of rats fed a cancer promoting methyl-deficient diet. *Carcinogenesis* 1991;12:1307-1312.
- Tsujiuchi T, Tsutsumi M, Sasaki Y, Takahama M, Konishi Y. Hypomethylation of CpG sites and c-myc gene overexpression in hepatocellular carcinomas, but not hyperplastic nodules, induced by a choline-deficient L-amino acid-defined diet in rats. *Jpn J Cancer Res* 1999;90:909-913.
- Alizadeh AA, Ross DT, Perou CM, van de RM. Towards a novel classification of human malignancies based on gene expression patterns. *J Pathol* 2001;195:41-52.
- Garber ME, Troyanskaya OG, Schluens K, Petersen S, Thaesler Z, Pacyna-Gengelbach M, et al. Diversity of gene expression in adenocarcinoma of the lung. *Proc Natl Acad Sci U S A* 2001;98:13784-13789.
- Sorlie T, Perou CM, Tibshirani R, Aas T, Geisler S, Johnsen H, et al. Gene expression patterns of breast carcinomas distinguish tumor subclasses with clinical implications. *Proc Natl Acad Sci U S A* 2001;98:10869-10874.
- Bertucci F, Finetti P, Rougemont J, Charafe-Jauffret E, Nasser V, Lloriod B, et al. Gene expression profiling for molecular characterization of inflammatory breast cancer and prediction of response to chemotherapy. *Cancer Res* 2004;64:8558-8565.
- Paules R. Phenotypic anchoring: linking cause and effect. *Environ Health Perspect* 2003;111:A338-A339.
- Denda A, Kitayama W, Murata A, Kishida H, Sasaki Y, Kusuoka O, et al. Increased expression of cyclooxygenase-2 protein during rat hepatocarcinogenesis caused by a choline-deficient, L-amino acid-defined diet and chemopreventive efficacy of a specific inhibitor, nimesulide. *Carcinogenesis* 2002;23:245-256.
- Irizarry RA, Hobbs B, Collin F, Beazer-Barclay YD, Antonellis KJ, Scherf U, et al. Exploration, normalization, and summaries of high density oligonucleotide array probe level data. *Biostatistics* 2003;4:249-264.
- Eisen MB, Spellman PT, Brown PO, Botstein D. Cluster analysis and display of genome-wide expression patterns. *Proc Natl Acad Sci U S A* 1998;95:14863-14868.
- Sorlie T, Tibshirani R, Parker J, Hastie T, Marron JS, Nobel A, et al. Repeated observation of breast tumor subtypes in independent gene expression data sets. *Proc Natl Acad Sci U S A* 2003;100:8418-8423.
- Tusher VG, Tibshirani R, Chu G. Significance analysis of microarrays applied to the ionizing radiation response. *Proc Natl Acad Sci U S A* 2001;98:5116-5121.
- Rusyn I, Denissenko MF, Wong VA, Butterworth BE, Cunningham ML, Upton PB, et al. Expression of base excision repair enzymes in rat and mouse liver is induced by peroxisome proliferators and is dependent upon carcinogenic potency. *Carcinogenesis* 2000;21:2141-2145.
- Nakamura J, La DK, Swenberg JA. 5'-nicked apurinic/aprimidinic sites are resistant to β -elimination by β -polymerase and are persistent in human cultured cells after oxidative stress. *J Biol Chem* 2000;275:5323-5328.
- Nakamura J, Swenberg JA. Endogenous apurinic/aprimidinic sites in genomic DNA of mammalian tissues. *Cancer Res* 1999;59:2522-2526.
- Zielinska-Park J, Nakamura J, Swenberg JA, Aitken MD. Aldehydic DNA lesions in calf thymus DNA and HeLa S3 cells produced by bacterial quinone metabolites of fluoranthene and pyrene. *Carcinogenesis* 2004;25:1727-1733.
- Khatri P, Bhavsar P, Bawa G, Draghici S. Onto-Tools: an ensemble of web-accessible, ontology-based tools for the functional design and interpretation of high-throughput gene expression experiments. *Nucleic Acids Res* 2004;32:W449-W456.
- Lombardi B, Pani P, Schlunk FF. Choline-deficiency fatty liver: impaired release of hepatic triglycerides. *J Lipid Res* 1968;9:437-446.
- Nishizuka Y. Studies and perspectives of protein kinase C. *Science* 1986; 233:305-312.
- Weinstein IB. The role of protein kinase C in growth control and the concept of carcinogenesis as a progressive disorder in signal transduction. *Adv Second Messenger Phosphoprotein Res* 1990;24:307-316.
- Yen CL, Mar MH, Craciunescu CN, Edwards LJ, Zeisel SH. Deficiency in methionine, tryptophan, isoleucine, or choline induces apoptosis in cultured cells. *J Nutr* 2002;132:1840-1847.
- Lotersztajn S, Julien B, Teixeira-Clerc F, Grenard P, Mallat A. Hepatic fibrosis: molecular mechanisms and drug targets. *Annu Rev Pharmacol Toxicol* 2004.
- Kershenovich SD, Weissbrod AB. Liver fibrosis and inflammation: a review. *Ann Hepatol* 2003;2:159-163.
- Iredale JP, Murphy G, Hembry RM, Friedman SL, Arthur MJ. Human hepatic lipocytes synthesize tissue inhibitor of metalloproteinases-1. Implications for regulation of matrix degradation in liver. *J Clin Invest* 1992; 90:282-287.
- Herbst H, Wege T, Milani S, Pellegrini G, Orzechowski HD, Bechstein WO, et al. Tissue inhibitor of metalloproteinase-1 and -2 RNA expression in rat and human liver fibrosis. *Am J Pathol* 1997;150:1647-1659.
- Zeeberg BR, Feng W, Wang G, Wang MD, Fojo AT, Sunshine M, et al. GoMiner: a resource for biological interpretation of genomic and proteomic data. *Genome Biol* 2003;4:R28.
- Rusyn I, Asakura S, Pachkowski B, Bradford BU, Denissenko MF, Peters JM, et al. Expression of base excision DNA repair genes is a sensitive biomarker for in vivo detection of chemical-induced chronic oxidative stress: identification of the molecular source of radicals responsible for DNA damage by peroxisome proliferators. *Cancer Res* 2004;64:1050-1057.

36. Lopatina NG, Vanyushin BF, Cronin GM, Poirier LA. Elevated expression and altered pattern of activity of DNA methyltransferase in liver tumors of rats fed methyl-deficient diets. *Carcinogenesis* 1998;19:1777-1781.
37. Wakasugi N, Tagaya Y, Wakasugi H, Mitsui A, Maeda M, Yodoi J, et al. Adult T-cell leukemia-derived factor/thioredoxin, produced by both human T-lymphotropic virus type I- and Epstein-Barr virus-transformed lymphocytes, acts as an autocrine growth factor and synergizes with interleukin 1 and interleukin 2. *Proc Natl Acad Sci U S A* 1990;87:8282-8286.
38. European Standards Committee on Oxidative DNA Damage (ES-CODD). Measurement of DNA oxidation in human cells by chromatographic and enzymic methods. *Free Radic Biol Med* 2003;34:1089-1099.
39. ESCODD. Measurement of DNA oxidation in human cells by chromatographic and enzymic methods. *Free Radic Biol Med* 2003;34:1089-1099.
40. Yoshiji H, Nakae D, Mizumoto Y, Horiguchi K, Tamura K, Denda A, et al. Inhibitory effect of dietary iron deficiency on inductions of putative preneoplastic lesions as well as 8-hydroxydeoxyguanosine in DNA and lipid peroxidation in the livers of rats caused by exposure to a choline-deficient L-amino acid defined diet. *Carcinogenesis* 1992;13:1227-1233.
41. Cheng KC, Cahill DS, Kasai H, Nishimura S, Loeb LA. 8-Hydroxyguanine, an abundant form of oxidative DNA damage, causes G→T and A→C substitutions. *J Biol Chem* 1992;267:166-172.
42. Luczaj W, Skrzydlewska E. DNA damage caused by lipid peroxidation products. *Cell Mol Biol Lett* 2003;8:391-413.
43. Zindy P, Andrieux L, Bonnier D, Musso O, Langouet S, Campion JP, et al. Upregulation of DNA repair genes in active cirrhosis associated with hepatocellular carcinoma. *FEBS Lett* 2005;579:95-99.
44. Jungst C, Cheng B, Gehrke R, Schmitz V, Nischalke HD, Ramakers J, et al. Oxidative damage is increased in human liver tissue adjacent to hepatocellular carcinoma. *HEPATOLOGY* 2004;39:1663-1672.
45. Chen X, Cheung ST, So S, Fan ST, Barry C, Higgins J, et al. Gene expression patterns in human liver cancers. *Mol Biol Cell* 2002;13:1929-1939.